Geophysical Research Letters

Supporting Information for

Warmer, wetter climates accelerate mechanical weathering in field data, independent of stress-loading

[1]MC Eppes, [1]B. Magi, [1]J. Scheff, [2]K. Warren, [1]S. Ching, [1]T. Feng

Corresponding author: Martha Cary (Missy) Eppes (meppes@uncc.edu)

[1] Department of Geography & Earth Sciences, University of North Carolina at Charlotte, 9201 University City Blvd., Charlotte, NC 28223

[2]Department of Civil and Environmental Engineering, University of North Carolina at Charlotte, 9201 University City Blvd., Charlotte, NC 28223

Contents of this file

Additional Supporting Information (Files uploaded separately)

Introduction

This file contains supplemental figures and tables as described in the Main Text. All analyses in the main text and this supplement are derived from the Hourly Datasets provided in the supporting material for this paper.

The NM and NC Hourly Data files are datasets of hourly weather and acoustic emission data collected in North Carolina (NC) and New Mexico (NM). Details of all data collection and QC and production of the dataset are described in Warren et al., 2013; Eppes et al. 2016; and Ching, 2018 and the main text. The Freezing Time Data files are a list of all dates in the respective datasets that experienced any (i.e. >0 minutes) of freezing air temperatures. This Freezing filter is applied to all data presented in the main text and supplement.

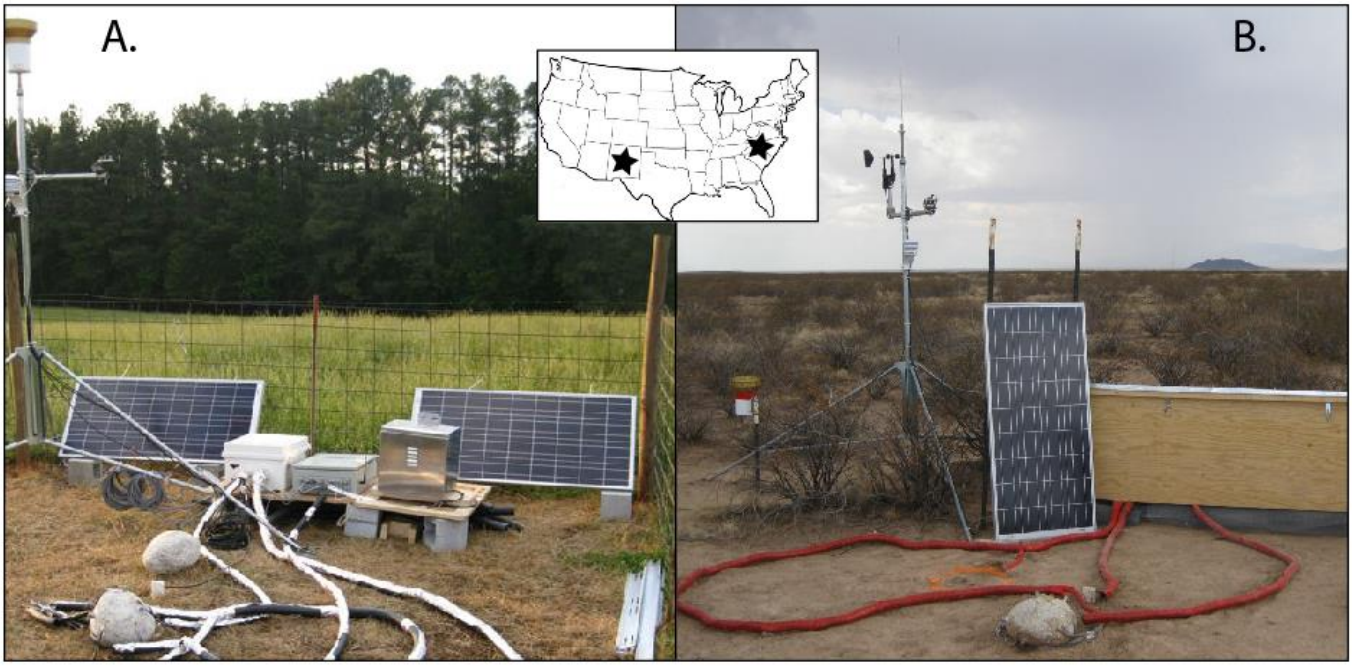

Figure S1. Photographs of the instrumented boulders. A) North Carolina and B) New Mexico. The 2nd boulder visible in the NC photograph was used to measure porosity and thermal diffusivity of the rock type represented by all three boulders.

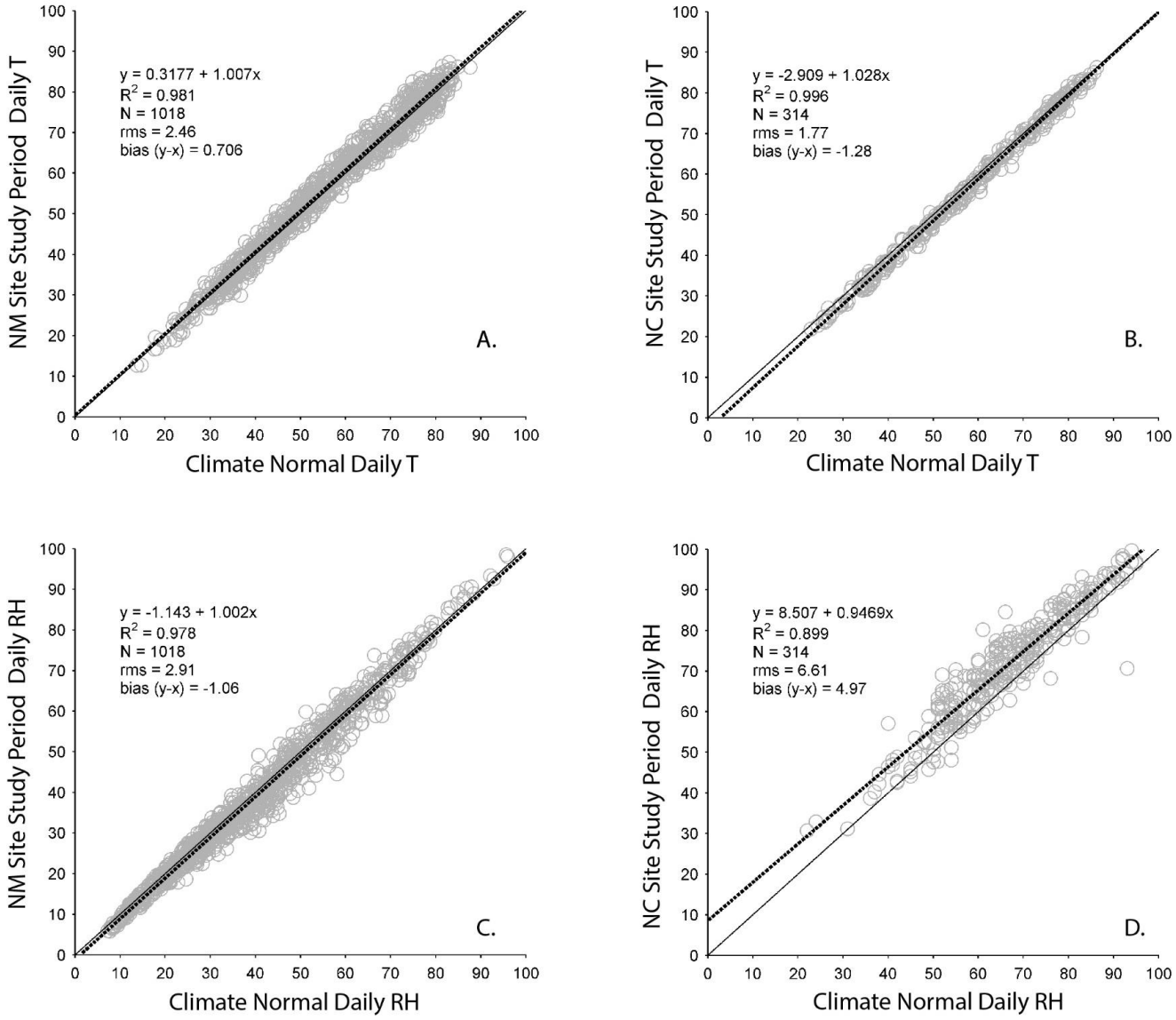

Figure S2. Comparisons of daily-averaged T and RH. Comparisons are between T & RH data measured at the weather stations co-located with the boulders in NM (left column) and NC (Right Column) with T and RH measured by nearby (<~20km) weather stations at Gastonia Airport (KAKH) and LTER Station 40 in order to determine to what extent the monitoring years deviated from 'normal' climate conditions. Statistics include equation of best fit line, coefficient of determination (R^2), number of data points (N), root mean squared difference (rms), and mean bias (bias). The dashed line is the regression, and the solid line is the one-to-one line.

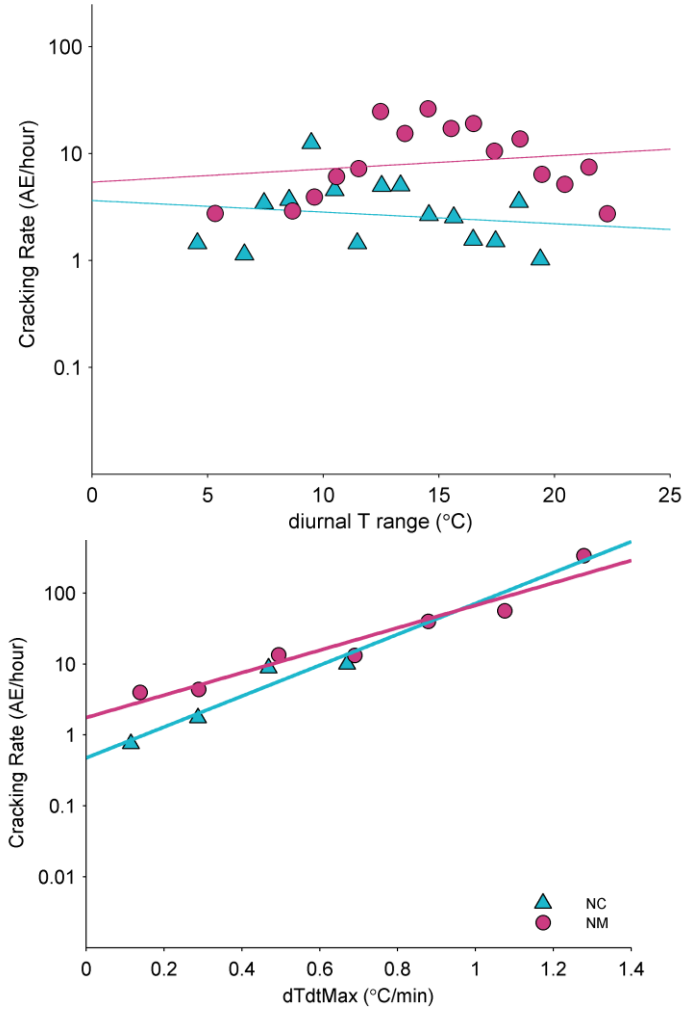

Figure S3. Cracking rate (average AE events per hour) for bins of stress magnitude proxies diurnal temperature range (diurnal T range; top) and the hourly maximum rate of per minute change (dT/dt Max; bottom). Calculated for the NM (pink) and NC (blue) boulders as a function of (A.) the maximum-minimum average hourly T in a 24 hour day (diurnal T range °C) averaged in bins of $1^{\circ}C$ at each site, and (B.) measured hourly maximum rate of per minute change (bins of 0.1 °C/min, dT/dtMax).

We note the lack of correlation for diurnal T range is possibly due to low numbers of days with events.

dT/dt Max directly correlates with cracking in both datasets as would be expected given their influence on thermal stresses (Ravaji et al., 2019). In general, published work shows dT/dt scales with thermal stresses in rock masses because the magnitude of the thermal stresses arising during heating or cooling of a rock mass are proportional to the contrast between the rate of T change between different regions of the rock mass (Ravaji et al., 2019). Fast rates of temperature change in the atmosphere will translate to fast changes at the rock surface compared to its interior, thus higher experienced rock stress magnitude for a given air dT/dt, thus faster cracking.

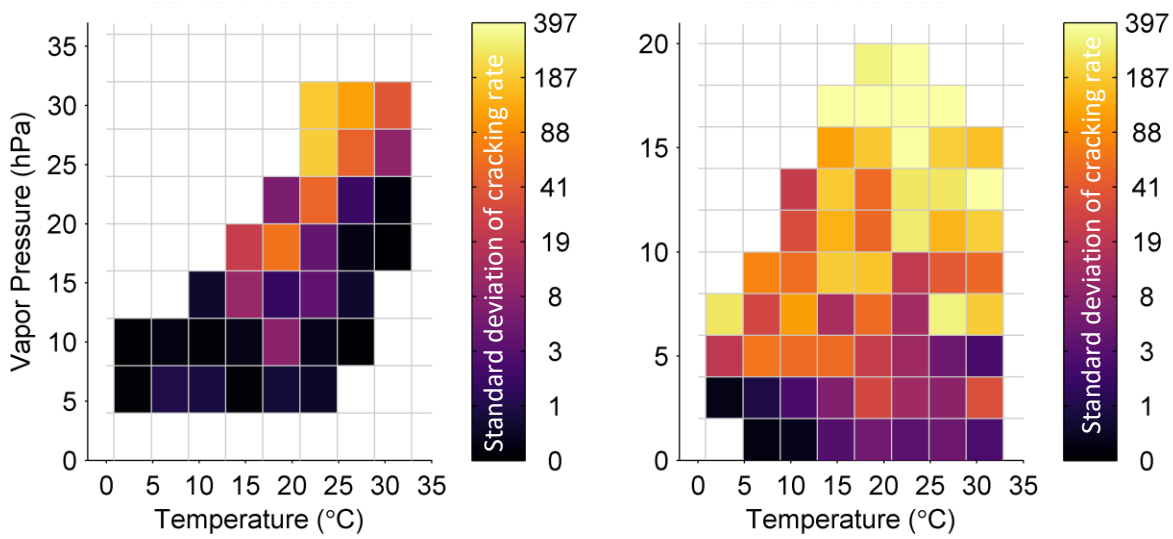

Figure S4. As Fig. 2 in the main text, but plotting the standard deviation of cracking rate (AE/hr) in each bin.

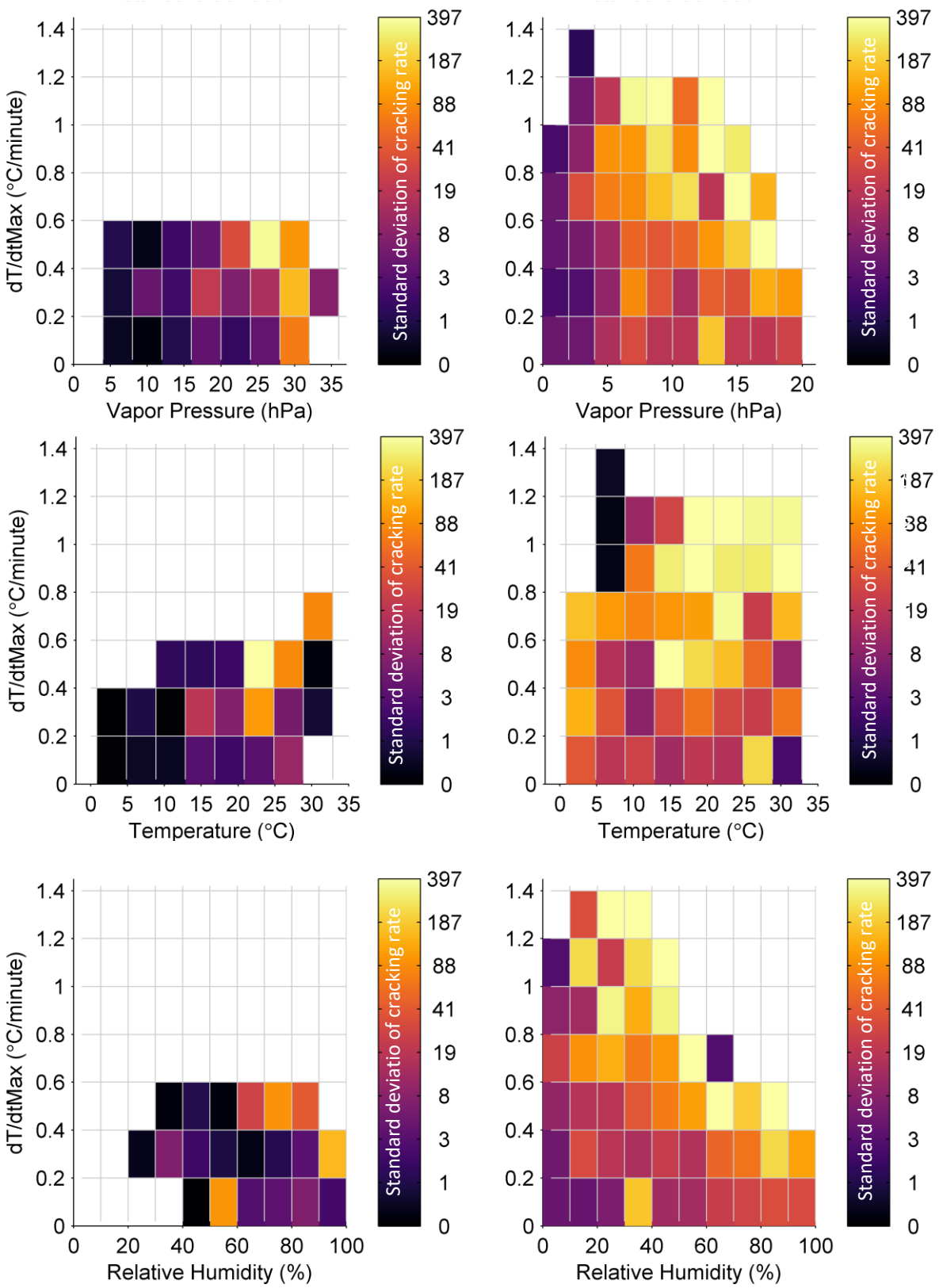

Figure S5. As Fig. 3 in the main text, but plotting the standard deviation of cracking rate (AE/hr) in each bin.

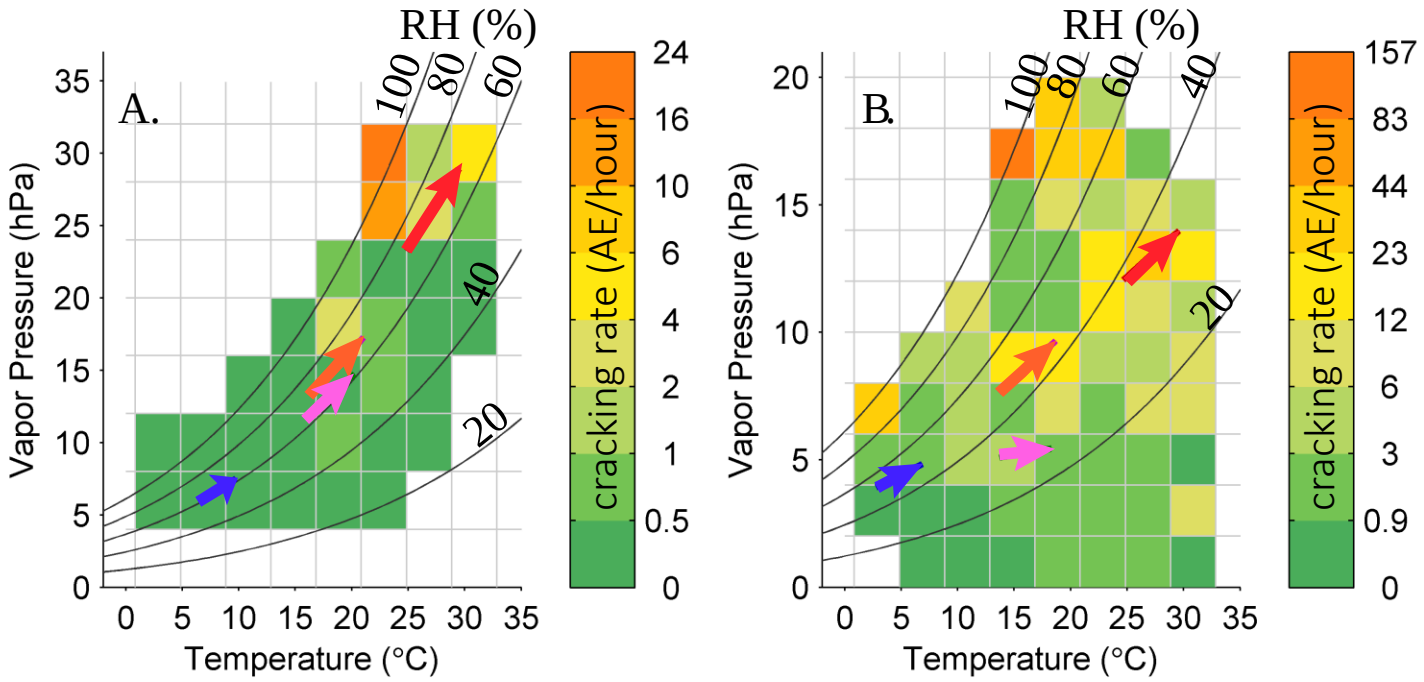

Figure S6. Analogous plots to Fig. 2 in the text, but where all hours in which rain commenced are removed from the data. The figure depicts rock cracking rate (AE events per hour – color scales) as a function of measured hourly average ambient VP (bins of 4 hPa) and temperature (bins of 4 °C) for the boulder in (A.) NC and (B.) NM. Lines of constant RH are overlaid in black.

Eppes et al. (2016) and Ching (2018) determined that a significant fraction of cracking in both the NC and NM data occurs during periods of high thermal stresses brought on by rapid cooling caused by the onset of rain. To test the sensitivity of results to such rain-induced temperature change, in this plot we excluded all hours in which rainfall commenced from the analysis. The correlations between cracking rate and VP remain dominant for all datasets (Tables S3 & S4) suggesting that the strong relationships between VP and cracking are not an artifact of the onset of rain as a primary mechanism of inducing thermal stress loading.

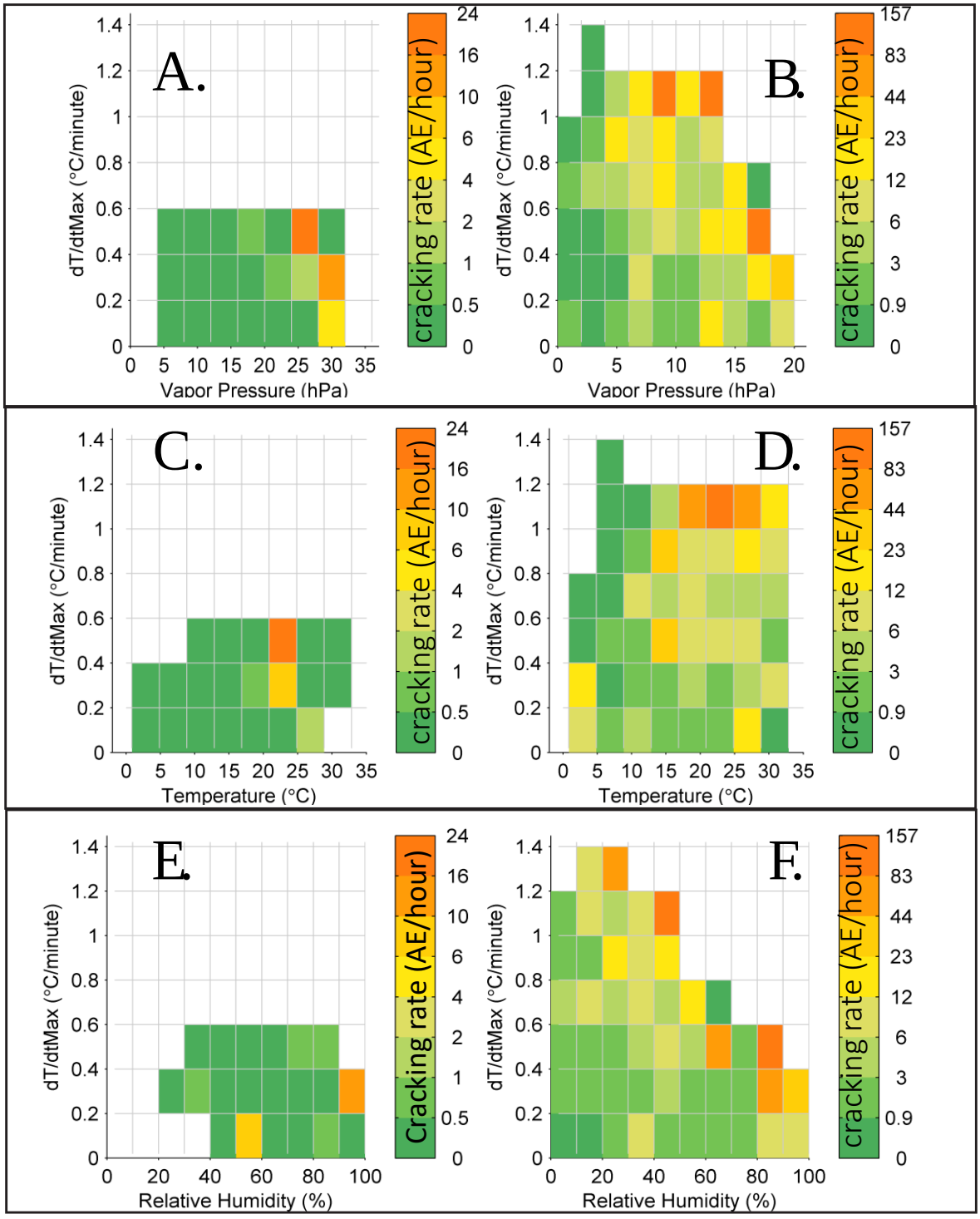

Figure S7. Analogous plots to Fig. 3 in the text, but where all hours in which rain commenced are removed from the data. Hourly cracking rate as a function of hourly maximum rate of temperature change (dT/dt Max, °C /minute); versus (A. and B.) RH (C. and D.) temperature and (E. and F.) VP. Left graphs are North Carolina; right are New Mexico.

Eppes et al. (2016) and Ching (2018) determined that a significant fraction of cracking in both the NC and NM data occurs during periods of high thermal stresses brought on by rapid cooling caused by the onset of rain. To test the sensitivity of results to such rain-induced temperature change, in this plot we excluded all hours in which rainfall commenced from the analysis. The correlations between cracking rate and VP remain dominant for all datasets (Tables S3 & S4) suggesting that the strong relationships between moisture and cracking are not an artifact of the onset of rain as a primary mechanism of inducing thermal stress loading.

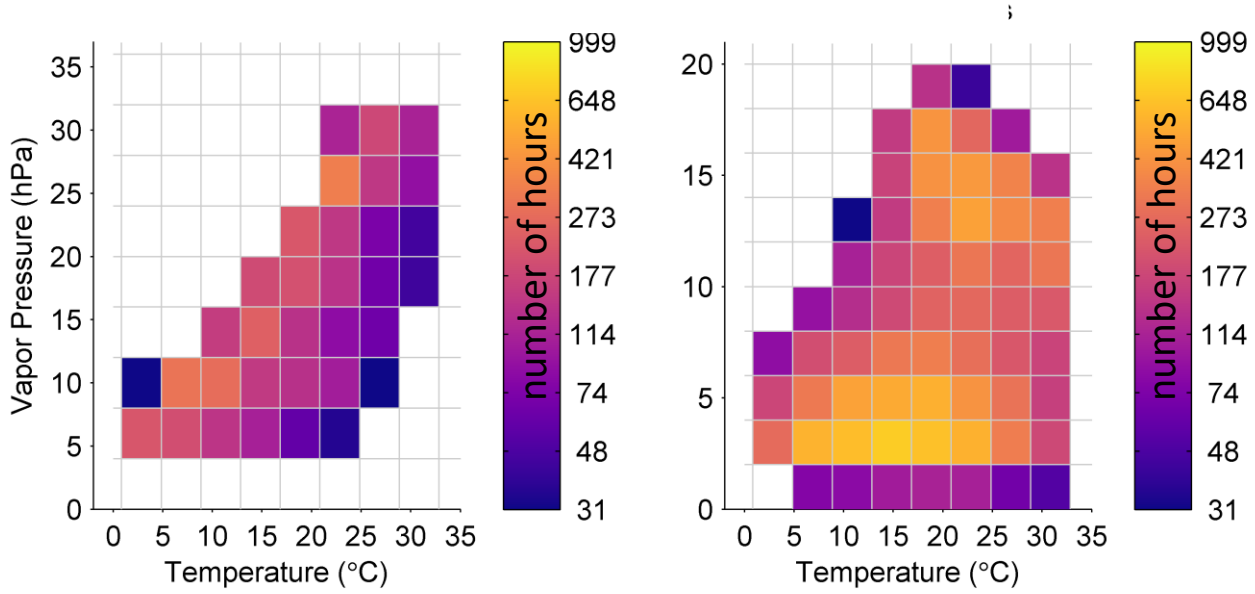

Figure S8. As Fig. 2 in the main text, but plotting the total number of hours of data included in the calculation (Figs. 2 and S4) for each bin. NC – left; NM – right.

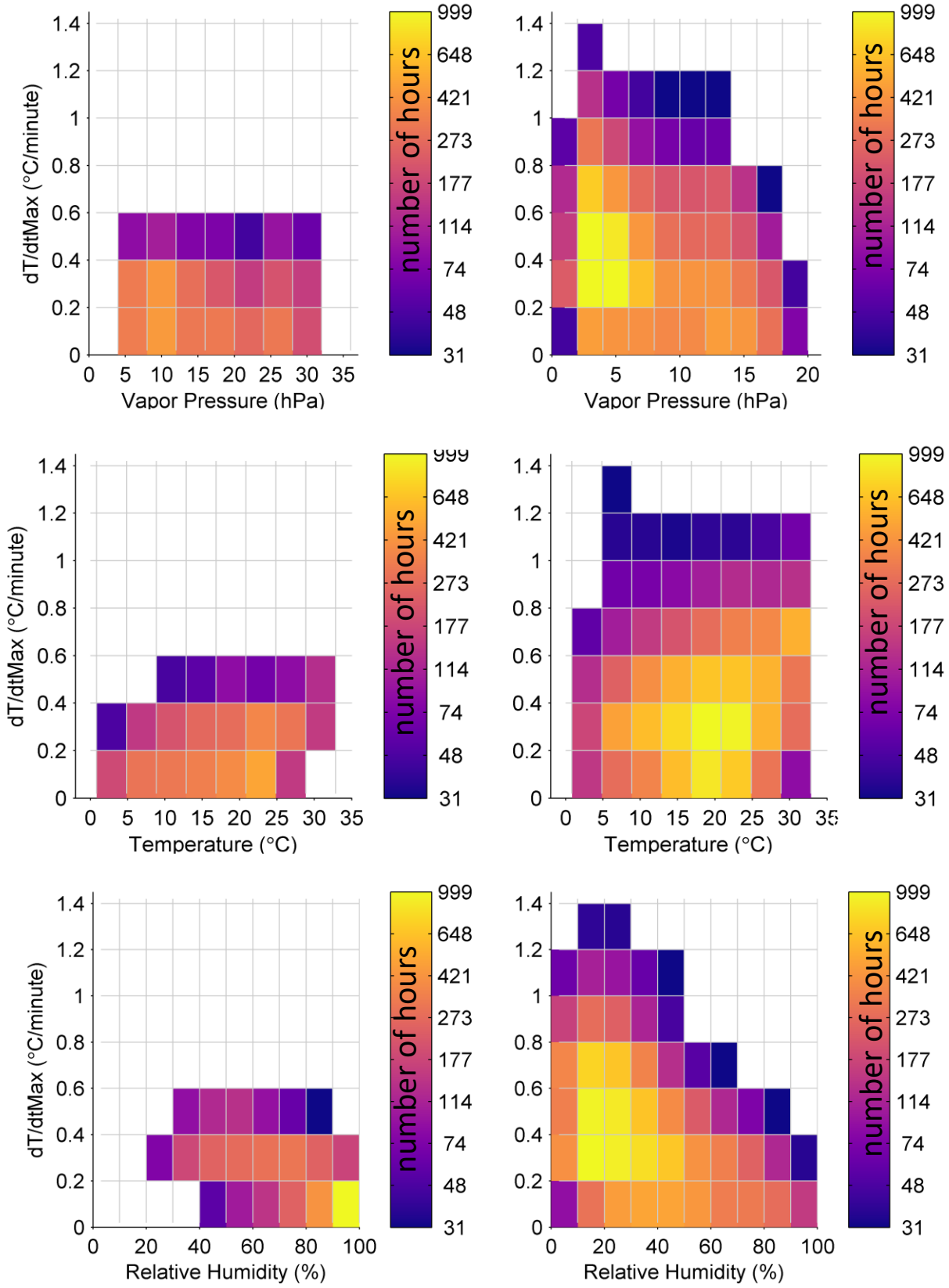

Figure S9. As Fig. 3 in the main text, but plotting the total number of hours of data included in the calculations (Figs. 3 and S5) for each bin. NC – left; NM – right.

Fig. 1 Stats	Cracking rate (AE/hour) vs VP (hPa)		Cracking rate (AE/hour) vs T (°C)		Cracking rate (AE/hour) vs RH (%)	
	NC	NM	NC	NM	NC	NM
r	0.88	0.97	0.82	0.69	0.87	0.70
p	7.54E-05	8.79E-05	1.11E-03	9.28E-03	5.13E-03	2.28E-02
intercept	-1.9174	-0.0130	-30.0517	-12.8530	-1.7755	0.6620
intercept error	0.3277	0.1362	6.5594	4.3768	0.4406	0.2218
slope	0.0962	0.1110	0.1022	0.0477	0.0293	0.0109
slope error	0.0157	0.0119	0.0226	0.0151	0.0068	0.0039
N	13	8	12	13	8	10
Doubling of cracking rate	3.13	2.71	2.95	6.31	10.27	27.73
Fig. S3 Stats	Cracking rate (AE/hour) vs dT/dt Diurnal		Cracking rate (AE/hour) vs dT/dt Max			
	NC	NM	NC	NM		
r	-0.27	0.017	0.82	0.69		
p	0.25	0.936	1.11E-03	9.28E-03		
intercept	0.748	0.878	-30.0517	-12.8530		
intercept error	0.325	0.351	6.5594	4.3768		
slope	-0.0156	0.001	0.1022	0.0477		
slope error	0.0129	0.0123	0.0226	0.0151		
N	20	25	12	13		

Table S1. Statistics from bivariate cracking rate correlations in Fig. 1 and Fig. S3. Data were processed with a minimum of 24 hours of sampling per depicted bin. All minutes within each sampled day were characterized by T > 0 °C. See Main Text for additional details of calculations. N refers to total number of bins in the regression. The doubling of the cracking rate refers to the metric in question such that, for example, the cracking rate doubles for every 3.13 hPa increase in VP in NC, and so on.

	NC winter	NC spring	NC summer	NC fall		NM winter	NM spring	NM summer	NM fall
T (°C)	6.4	16.0	24.9	16.3		2.8	13.7	24.7	13.7
ΔT	+3.3	+4.2	+4.6	+4.7		+4.1	+4.6	+4.9	+5.0
T+ΔT	9.7	20.2	29.5	21.0		6.8	18.3	29.6	18.7
RH (%)	62.5	64.3	72.5	71.6		52.5	32.2	38.1	48.5
ΔRH	-0.6	-3.0	-4.1	-3.2		-3.8	-6.6	-5.2	-4.1
RH+ΔRH	61.9	61.3	68.4	68.4		48.6	25.6	32.9	44.4
VP (hPa)	6.0	11.8	23.3	13.4		3.9	5.1	12.1	7.6
ΔVP	+1.5	+2.9	+5.7	+3.9		+0.9	+0.4	+1.9	+2.0
VP+ΔVP	7.5	14.7	28.9	17.3		4.8	5.4	14.0	9.7

Table S2. CMIP5-median local projected changes in T and RH applied to observed climate at the NC and NM sites (Depicted as arrows in Figs. 2 & S6). Changes may appear not to add exactly, due to rounding.

Correlation Statistics for Fig. 2

NC

T bin (°C)	Correlation of CR with VP	# of VP bins used
9-13	-0.01	3
13-17	**0.95**	**4**
17-21	0.47	5
21-25	**0.94**	**7**
25-29	**0.88**	**6**
29-33	0.94	4

CR v. VP

NM

T bin (°C)	Correlation of CR with VP	# of VP bins used
1-5	0.97	3
5-9	**0.94**	**5**
9-13	**0.75**	**7**
13-17	**0.88**	**9**
17-21	**0.90**	**10**
21-25	**0.95**	**10**
25-29	**0.87**	**9**
29-33	**0.77**	**8**

NC

VP bin (hPa)	Correlation of CR with T	# of T bins used
4-8	0.21	6
8-12	0.22	7
12-16	0.02	5
16-20	-0.80	5
20-24	-0.46	4
24-28	-0.99	3
28-32	-0.94	3

CR v. T

NM

VP bin (hPa)	Correlation of CR with T	# of T bins used
0-2	0.72	7
2-4	**0.94**	**8**
4-6	**-0.78**	**8**
6-8	-0.08	8
8-10	-0.63	7
10-12	0.55	6
12-14	0.69	6
14-16	0.32	5
16-18	0.01	4

Correlation Statistics for Fig. S6

NC

T bin (°C)	Correlation of CR with VP	# of VP bins used
9-13	0.02	3
13-17	0.94	4
17-21	0.45	5
21-25	**0.81**	**7**
25-29	0.74	6
29-33	0.94	4

CR v. VP

NM

T bin (°C)	Correlation of CR with VP	# of VP bins used
1-5	0.98	3
5-9	**0.99**	**5**
9-13	**0.90**	**6**
13-17	0.56	9
17-21	**0.71**	**10**
21-25	**0.63**	**10**
25-29	0.46	9
29-33	0.52	8

NC

VP bin (hPa)	Correlation of CR with T	# of T bins used
4-8	0.72	6
8-12	0.23	7
12-16	0.33	5
16-20	-0.50	5
20-24	-0.83	4
24-28	**-1.00**	**3**
28-32	-0.63	3

CR v. T

NM

VP bin (hPa)	Correlation of CR with T	# of T bins used
0-2	0.72	7
2-4	**0.93**	**8**
4-6	-0.51	8
6-8	-0.14	8
8-10	0.18	7
10-12	0.19	6
12-14	0.80	5
14-16	0.53	5
16-18	-0.88	4

Table S3. Pearson r values between cracking rate (CR) and the indicated variable, for cracking that occurred under a limited range (bin) of T or VP conditions (i.e. within a single row or column on the indicated figure). Correlations whose p-values are <0.05 are in bold. Negative correlations are in red. Fig. S6 reflects the same data as Fig. 2 except all hours in which rain commenced have been removed from the data for the analysis. In both analyses, positive correlations are stronger for CR v. VP than CR v. T.

Correlation Statistics for Fig. 3

NC

VP

dTdtMax bin (°C/min)	Correlation of CR with VP	# of VP bins used
0-0.2	0.74	7
0.2-0.4	**0.77**	**8**
0.4-0.6	**0.88**	**7**

VP bin (hPa)	Correlation of CR with dTdtMax	# of dTdtMax bins used
4-8	**0.99**	**3**
8-12	0.15	3
12-16	0.73	3
16-20	0.13	3
20-24	0.95	3
24-28	0.94	3
28-32	0.85	3

T

dTdtMax bin (°C/min)	Correlation of CR with T	# of T bins used
0-0.2	**0.87**	**7**
0.2-0.4	0.35	8
0.4-0.6	0.31	6

T bin (°C)	Correlation of CR with dTdtMax	# of dTdtMax bins used
9-13	0.79	3
13-17	-0.21	3
17-21	0.01	3
21-25	**1.00**	**3**
25-29	0.79	3
29-33	0.86	3

RH

dTdtMax bin (°C/min)	Correlation of CR with RH	# of RH bins used
0-0.2	-0.27	6
0.2-0.4	0.60	8
0.4-0.6	**0.90**	**6**

RH bin	Correlation of CR with dTdtMax	# of dTdtMax bins used
40-50	0.89	3
50-60	-0.88	3
60-70	0.74	3
70-80	0.84	3
80-90	0.86	3

NM

VP

dTdtMax bin (°C/min)	Correlation of CR with VP	# of VP bins used
0-0.2	**0.65**	**10**
0.2-0.4	**0.86**	**10**
0.4-0.6	**0.93**	**9**
0.6-0.8	**0.77**	**9**
0.8-1	**0.92**	**8**
1-1.2	0.80	6

VP bin (hPa)	Correlation of CR with dTdtMax	# of dTdtMax bins used
0-2	0.14	5
2-4	0.06	7
4-6	0.62	6
6-8	**0.88**	**6**
8-10	**0.97**	**6**
10-12	**0.89**	**6**
12-14	0.68	6
14-16	**0.98**	**5**
16-18	0.71	4

T

dTdtMax bin (°C/min)	Correlation of CR with T	# of T bins used
0-0.2	-0.20	8
0.2-0.4	-0.24	8
0.4-0.6	0.07	8
0.6-0.8	-0.20	8
0.8-1	0.70	7
1-1.2	**0.85**	**7**

T bin (°C)	Correlation of CR with	# of dTdtMax bins used
1-5	0.48	4
5-9	-0.59	7
9-13	0.26	6
13-17	0.47	6
17-21	**0.96**	**6**
21-25	**0.98**	**6**
25-29	0.61	6
29-33	**0.91**	**6**

RH

dTdtMax bin (°C/min)	Correlation of CR with RH	# of RH bins used
0-0.2	**0.66**	**10**
0.2-0.4	**0.90**	**10**
0.4-0.6	**0.91**	**9**
0.6-0.8	0.17	7
0.8-1	**0.93**	**5**
1-1.2	0.85	5

RH bin	Correlation of CR with dTdtMax	# of dTdtMax bins used
0-10	0.45	6
10-20	**0.78**	**7**
20-30	**0.84**	**7**
30-40	**0.83**	**7**
40-50	**0.98**	**6**
50-60	**0.95**	**4**
60-70	0.02	4
70-80	0.99	3
80-90	**0.99**	**3**

Correlation Statistics for Fig. S7

NC

VP

dTdtMax bin (°C/min)	Correlation of CR with VP	# of VP bins used
0-0.2	**0.70**	**7**
0.2-0.4	**0.80**	**7**
0.4-0.6	0.40	7

VP bin (hPa)	Correlation of CR with dTdtMax	# of dTdtMax bins used
4-8	0.91	3
8-12	0.18	3
12-16	-0.51	3
16-20	0.45	3
20-24	0.01	3
24-28	0.94	3
28-32	-0.72	3

T

dTdtMax bin (°C/min)	Correlation of CR with T	# of T bins used
0-0.2	**0.81**	**7**
0.2-0.4	0.34	8
0.4-0.6	0.12	6

T bin (°C)	Correlation of CR with dTdtMax	# of dTdtMax bins used
9-13	0.79	3
13-17	-0.85	3
17-21	-0.13	3
21-25	**1.00**	**3**
25-29	-0.87	3

RH

dTdtMax bin (°C/min)	Correlation of CR with RH	# of RH bins used
0-0.2	-0.30	6
0.2-0.4	0.56	8
0.4-0.6	0.74	6

RH bin	Correlation of CR with dTdtMax	# of dTdtMax bins used
40-50	0.89	3
50-60	-0.88	3
60-70	-0.89	3
70-80	0.43	3
80-90	0.06	3

NM

VP

dTdtMax bin (°C/min)	Correlation of CR with VP	# of VP bins used
0-0.2	0.56	10
0.2-0.4	**0.87**	**10**
0.4-0.6	**0.89**	**9**
0.6-0.8	0.01	9
0.8-1	0.65	7
1-1.2	**0.88**	**6**

VP bin (hPa)	Correlation of CR with dTdtMax	# of dTdtMax bins used
0-2	0.14	5
2-4	-0.03	7
4-6	0.64	6
6-8	0.53	6
8-10	**0.95**	**6**
10-12	0.78	6
12-14	0.55	6
14-16	**0.95**	**4**
16-18	0.04	4

T

dTdtMax bin (°C/min)	Correlation of CR with T	# of T bins used
0-0.2	-0.18	8
0.2-0.4	0.08	8
0.4-0.6	0.39	8
0.6-0.8	0.66	8
0.8-1	0.55	7
1-1.2	0.72	7

T bin (°C)	Correlation of CR with dTdtMax	# of dTdtMax bins used
1-5	-0.83	4
5-9	-0.74	7
9-13	-0.27	6
13-17	0.40	6
17-21	**0.88**	**6**
21-25	**0.84**	**6**
25-29	0.48	6
29-33	0.77	6

RH

dTdtMax bin (°C/min)	Correlation of CR with RH	# of RH bins used
0-0.2	0.61	10
0.2-0.4	0.74	10
0.4-0.6	**0.69**	**9**
0.6-0.8	-0.16	7
0.8-1	0.84	5
1-1.2	0.82	5

RH bin	Correlation of CR with dTdtMax	# of dTdtMax bins used
0-10	0.45	6
10-20	**0.86**	**7**
20-30	**0.85**	**7**
30-40	0.23	6
40-50	**0.84**	**6**
50-60	0.94	4
60-70	0.10	4
70-80	-0.68	3
80-90	**0.99**	**3**

Table S4. Pearson r values between cracking rate (CR) and the indicated variable, for cracking that occurred under a limited range (bin) of T, VP, RH and dT/dtMax conditions (i.e. within a single row or column on the indicated figure). Correlations whose p-values are <0.05 are in bold. Negative correlations are in red.
Fig. S7 reflects the same data as Fig. 3 except all hours in which rain commenced have been removed from the data for the analysis. In both analyses, positive correlations are stronger for CR v. VP than CR v. T or RH.

Dataset Captions

Dataset S1. Hourly NC Data. Ambient Temp, VaporPressure, and Relative-Humidity are hourly averages. Precipitation and AE are hourly sums.
dT/dt is the maximum rate of per minute temperature change within each hour.
Times with no data are listed as -999.

Dataset S2. Hourly NM Data. Ambient Temp, VaporPressure, and Relative-Humidity are hourly averages. Precipitation and AE are hourly sums.
dT/dt is the maximum rate of per minute temperature change within each hour.
Times with no data are listed as -999.

Dataset S3. NC Freezing Times. A list of the number of minutes in each day
Of the dataset that experienced temperatures <0C. This filter was applied for all analyses presented in the main text.
Times with no data are listed as -999.

Dataset S4. NM Freezing Times. A list of the number of minutes in each day
Of the dataset that experienced temperatures <0C. This filter was applied for all analyses presented in the main text.
Times with no data are listed as -999.